 

https://doi.org/10.1070/QEL17247

# Femtosecond dynamics of cavity modes in ZnSe films on a metal

E.A. Vinogradov

***Abstract.*** **The ultrafast evolution of cavity modes in a ZnSe film on a metal (Cr, Cu, or Ni) is studied by femtosecond pump/supercontinuum-probe spectroscopy on a time scale of several tens of femtoseconds. Femtosecond excitation of a microcavity in a ZnSe film on a metal substrate leads to a change in the parameters of cavity (Fabry–Perot) modes. The cavity-mode frequency shifts are due to the photoinduced changes in the boundary conditions and the optical thickness of microcavity.**

***Keywords:*** *femtosecond spectroscopy, semiconductor films, cavity mode, boundary conditions, permittivity, Schottky barrier.*

## 1. Introduction

Both physicists and technologists have long paid much attention to the optics of thin-film microcavity structures of the Fabry–Perot interferometer type. On the one hand, there is purely practical interest in such structures, which is related with the need to perform efficient control of laser radiation, i.e., develop a radically new element base for optoelectronics [1–5]. At the same time, using femtosecond laser pulses, one can manipulate the boundary conditions for microcavities and modify temporal, spectral, and spatial characteristics of chosen nanostructures [2–4]. This approach opens up new prospects for developing microcavity devices for optical data and image processing [1–3].

An insulator (semiconductor) film on an opaque metal substrate is a conventional mirror Fabry–Perot interferometer [6]. Its energy light transmittance $T(\omega)$ is zero. Thus, the energy conservation law

$$T(\omega) + R(\omega) + A(\omega) = 1, \tag{1}$$

where $R(\omega)$ and $A(\omega)$ are, respectively, the reflectance and absorptance (the light scattering is neglected), is reduced to the expression:

$$R(\omega) = 1 - A(\omega). \tag{2}$$

The reflectivity of this sample is unambiguously determined by its absorptivity. The spectra of the samples for which $T(\omega) = 0$ are referred to as reflection–absorption (RA) spectra. To determine $A(\omega)$ in this case, one must measure only one spectrum, $R(\omega)$, rather than two, as in the case $T(\omega) \neq 0$ [4, 5].

An interference mode – a cavity (microcavity) mode – is characterised by the dependence of frequency $\omega$ on the wave vector $\boldsymbol{k}$, even with the spatial dispersion effects disregarded. To reconstruct the dependence $\omega(\boldsymbol{k})$, one must measure reflection (absorption) spectra at different angles of incidence of light $\varphi$ on a film-on-substrate structure. The reflectance $R(\omega,\varphi)$ of a crystalline cavity of arbitrary thickness $d$ in a three-layer structure vacuum–semiconductor–metal film has the form [4, 5]

$$R = \left| \frac{(\delta_1 - \delta_2)(\delta_2 + \delta_3) + (\delta_1 + \delta_2)(\delta_2 - \delta_3)\exp(-2\kappa_2 d\omega/c)}{(\delta_1 + \delta_2)(\delta_2 + \delta_3) + (\delta_1 - \delta_2)(\delta_2 - \delta_3)\exp(-2\kappa_2 d\omega/c)} \right|^2, \tag{3}$$

where $\delta_j = \varepsilon_j/\kappa_j$ for p-polarised radiation and $\delta_j = \kappa_j$ for s-polarised radiation ($j$ = 1, 2, 3); $\kappa_j = [\varepsilon_1 \sin^2\varphi - \varepsilon_j(\omega)]^{1/2}$; $\varepsilon_1$ is the permittivity of free space;

$$\varepsilon_2(\omega) = \varepsilon_\infty - \Delta_\varepsilon + \frac{\Delta_\varepsilon \omega_{\rm ex}^2}{\omega_{\rm ex}^2 - \omega^2 - {\rm i}\gamma_{\rm ex}\omega} + \frac{(\varepsilon_0 - \varepsilon_\infty)\omega_{\rm TO}^2}{\omega_{\rm TO}^2 - \omega^2 - {\rm i}\gamma\omega} \tag{4}$$

is the film permittivity in the frequency range $\omega < \omega_{\rm ex}$; $\omega_{\rm ex} \approx E_{\rm g}/\hbar$ and $\gamma_{\rm ex}$ are, respectively, the exciton frequency and exciton damping constant; $E_{\rm g}$ is the semiconductor film band gap; $\Delta_\varepsilon$ is the exciton oscillator strength; $\omega_{\rm TO}$, $\gamma$ and $(\varepsilon_0 - \varepsilon_\infty)$ are, respectively, the frequency, damping constant, and oscillator strength of transverse optical phonon;

$$\varepsilon_3(\omega) = \varepsilon_{\rm m}(\omega) = \varepsilon_{\rm m\infty} - \frac{\omega_{\rm pm}^2}{\omega^2 - {\rm i}\gamma_{\rm pm}\omega} \tag{5}$$

is the metal substrate permittivity given by the Drude formula; $\omega_{\rm pm}$ and $\gamma_{\rm pm}$ are, respectively, the frequency and damping constant of plasma oscillations in the metal substrate; and $\varepsilon_{\rm m\infty}$ is the permittivity of metal at frequencies $\omega > \omega_{\rm pm}$.

The frequency and shape of the absorption band of cavity modes (radiative polaritons of the structure) are determined by the thickness and permittivity of the insulator film, while the absorption band intensities are determined by the value $\mathrm{Im}[\varepsilon_{\rm m}(\omega)]$ (i.e., the metal conductivity) [4, 5]. The intensity of the emission (absorption) band at the frequencies of interference modes of the plane-parallel insulator layer on a metal substrate increases with a decrease in the metal substrate conductivity. The light absorption may be due to the tails of the function of the density of phonon or electron (exciton) states

**E.A. Vinogradov** Institute for Spectroscopy, Russian Academy of Sciences, ul. Fizicheskaya 5, Troitsk, 108840 Moscow, Russia; e-mail: evinogr@isan.troitsk.ru

Received 24 December 2019
*Kvantovaya Elektronika* **50** (3) 246–251 (2020)
Translated by Yu.P. Sin'kov

of the film bulk and surface, density of multiphonon states, structural defects, or damping of plasma oscillations in the metal substrate. An initially nonradiative surface plasmon of metal at the metal–vacuum interface is partially transformed by the semiconductor (insulator) film on metal into a radiative plasmon: interference modes of the film on metal. And, even if the insulator film material does not absorb light ($\gamma_{ex} = \gamma = 0$), the interferometer absorbs and emits electromagnetic waves. The film in this structure can also be considered as a cavity for electromagnetic field (in particular, for vacuum), and the interference and waveguide modes can be regarded as cavity modes interacting with the plasmon of a cavity metal wall [4, 5].

Figure 1 (top) presents conventional spectra of linear absorption of light at interference mode frequencies in a 820-nm-thick ZnSe film on a thick (opaque) chromium film coating a quartz plate. The frequencies of the maxima of absorption bands in these spectra correspond to the cavity mode frequencies, and their FWHM determines the radiative decay time of cavity modes, as well as the effective number of interfering beams in the Fabry–Perot interferometer [4–6].

An excitation of this structure by laser radiation leads to a photoinduced change in the permittivity of both the semiconductor film and metal substrate. A change in the film permittivity leads to a change in the film optical thickness, while a change in the metal substrate permittivity changes the boundary conditions for interference modes in the film. Both these effects lead to a change in the frequency and shape of the interference-mode absorption band [4]. The half-width of this band is determined by the time of cavity mode decay (anharmonic and radiative). In the spectral region where the film is transparent, the contribution of anharmonic processes to the cavity mode decay is negligible in comparison with that of radiative processes. For a 820-nm-thick ZnSe film in the visible spectral range, at frequencies lower than the Wannier–Mott exciton frequencies but much higher than the optical phonon frequencies, the cavity mode radiative lifetime is ~100 fs [4]. This time is much shorter than the generation and relaxation times of any collective excitations (excitons and phonons) in the film material (which is on the order of several units or tens of picoseconds) but is comparable with the plasma oscillation settling time in metals.

The photoinduced response of the structure of ZnSe semiconductor film on a metal substrate was studied by femtosecond pump/supercontinuum-probe spectroscopy [4, 7–15]. The results of this study demonstrated the possibility of recording photoinduced ultrafast processes at the metal–semiconductor interface (in particular, due to the changes in permittivity) with a temporal resolution of several tens of femtoseconds. The aforementioned photoinduced responses in the femtosecond range were found to be most pronounced in the ultrafast evolution of interference modes (optical cavity modes in the ZnSe film).

The planar microcavity structures were (160–820)-nm-thick ZnSe filma deposited on thick (opaque in the visible spectral range) metal (Cr, Ni, or Cu) films [4, 7–15]. The ZnSe band gap at room temperature is $E_g \approx 2.7$ eV. Excitation was performed by optical pump pulses with photon energies $\hbar\omega_{p1} = 5.5$ eV, $\hbar\omega_{p2} = 2.75$ eV, $\hbar\omega_{p3} = 2.34$ eV and duration $\tau \approx 50$ fs. The pump pulse energy was varied in the range of 0.4–2 μJ. The supercontinuum (1.6–3.2 eV) probe pulse was dispersed by a polychromator with a resolution of ~1 nm. Probe pulses were delayed relative to the excitation pulse using an optical delay line; the delay time varied from –0.2 to +2.5 ps. The cross-correlation time of the pump–probe process was ~70 fs (FWHM) at all probe wavelengths. The probe spot diameter (~100 μm) was one and a half times smaller than the pump spot diameter. The RA spectra of supercontinuum probe pulse were recorded using a grating monochromator equipped with two high-speed diode CCD line arrays (1024 pixels). The optical density $D_R(\hbar\omega) = -\lg[R(\hbar\omega)]$ at different delay times $t_d$ was determined from the RA spectra. The difference in the optical density spectra $\Delta D_R(\hbar\omega) = -\lg[R(\hbar\omega)]$ of the excited and unexcited samples was analysed. Previous studies [4, 7–15] showed that the effect of pump pulse on the behaviour of cavity modes depends on the ratio of the pump photon energy $\hbar\omega_p$ to the semiconductor band gap $E_g$. Let us consider separately the supraband ($\hbar\omega_p > E_g$) and subband ($\hbar\omega_p < E_g$) excitation modes.

## 2. Supraband excitation ($\hbar\omega_p > E_g$)

In this case a laser pulse is absorbed in a thin surface semiconductor layer and generates a nonuniform distribution of hot carriers in the semiconductor. The occurrence of nonequilibrium carriers in the semiconductor layer, which is caused by the occupation of states in the conduction band and depletion of states in the valence band, changes the semiconductor permittivity (causes screening of exciton transitions and even photoinduced disappearance of exciton states). The increase in the free-carrier concentration at the light penetration depth in ZnSe changes the boundary conditions for the cavity modes and the permittivity $\varepsilon_2(\omega)$ of the semiconductor film near the absorption edge ($\hbar\omega \approx E_g$) and, therefore, causes a frequency shift of ZnSe cavity modes due to the decrease in the optical cavity thickness $nd$ ($n$ is the cavity refractive index) in the frequency range $\omega < \omega_{ex}$.

Figure 1 shows as an example the spectra $\Delta D_R(\hbar\omega)$ of a 820-nm-thick ZnSe film on an opaque chromium film for delay times in the range from –0.04 to 2.4 ps. The spectra $\Delta D_R(\hbar\omega)$ of a 820-nm ZnSe film on other metal substrates (Ni or Cu) do not differ radically from the spectra presented in Fig. 1. At the energy $\hbar\omega_{p1} = 5.5$ eV, excitation pulse energy 1.2 μJ, and pump spot diameter ~250 μm, no nonlinear effects were found and no fundamental differences in the temporal dynamics of the spectra $\Delta D_R(\hbar\omega)$ of ZnSe film on metal (chromium, nickel, or copper) substrates were observed. In this 'thick' ZnSe film, light with excitation photon energy $\hbar\omega_{p1} = 5.5$ eV is absorbed in the ZnSe surface layer and can barely reach the metal substrate.

The temporal dynamics of the spectrum $\Delta D_R(\hbar\omega)$ was determined by changing (with a step of 7 fs) the delay time between the excitation and probe pulses [7–15]. It can be seen in Fig. 1 that the intensity of the spectrum $\Delta D_R(\hbar\omega)$ changes maximally at the frequencies of optical cavity modes in the ZnSe film on chromium. The spectral region under consideration contains four cavity modes with different temporal dynamics (Fig. 1). The nonequilibrium carriers excited in a thin surface semiconductor layer relax due to the electron–phonon and electron–electron interactions and penetrate the unexcited part of the semiconductor. The temporal evolution of the semiconductor permittivity is determined by these processes [9].

The spectrum of the 250-nm-thick ZnSe film on chromium [15], in the case of its excitation with pulses characterised by the photon energy $\hbar\omega_p = 3.14$ eV (rather than 5.5 eV,

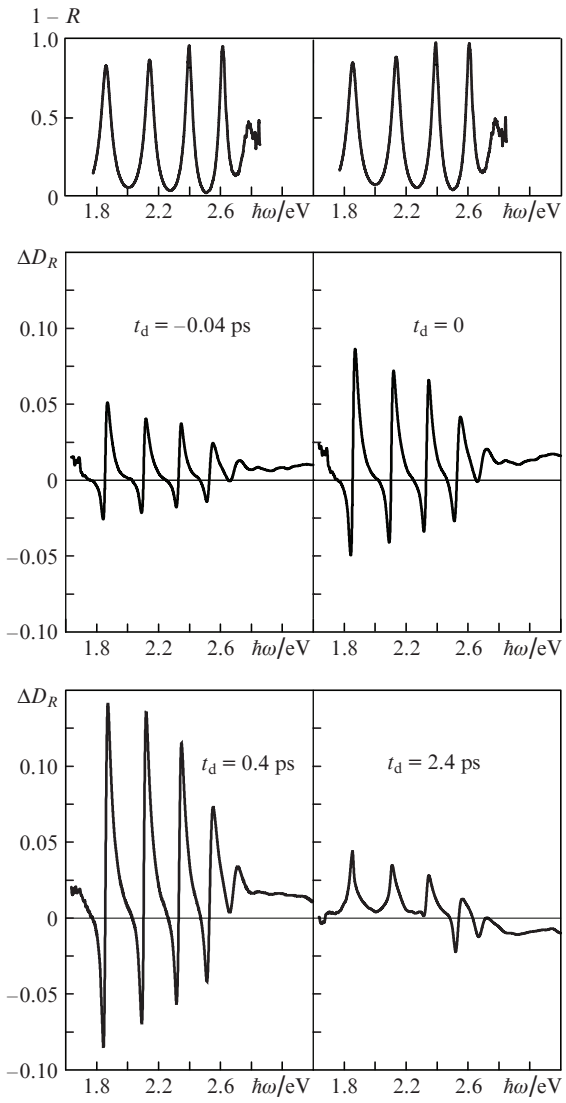


**Figure 1.** RA spectra (top) of a 820-nm-thick ZnSe film on an opaque chromium film on a quartz plate and the spectra $\Delta D_R(\hbar\omega)$ of this film at different delay times $t_d$. The pump photon energy $\hbar\omega_{p1}$ = 5.5 eV, the excitation pulse energy is 1.2 μJ, and the pump spot diameter is ~250 μm [7–9].

as in the above-considered case) and probing near the frequency of the interference mode absorption band, exhibits a fast maximum red shift of the cavity mode frequency for a time of ~200 fs rather than ~400 fs, as in the case of 820-nm-thick ZnSe film excited with a photon energy $\hbar\omega_p$ = 5.5 eV. The subsequent return of the peak of cavity mode absorption band to the initial (prior to excitation) position occurs in both cases for the same time (~20 ps).

Figure 2 shows the spectra $\Delta D_R(\hbar\omega)$ of 820-nm-thick ZnSe film on chromium at three pump photon energies: $\hbar\omega_{p1}$ = 5.5 eV, $\hbar\omega_{p2}$ = 2.75 eV, and $\hbar\omega_{p3}$ = 2.34 eV. The pumping with $\hbar\omega_{p2}$ = 2.75 eV leads to excitation of not only interband transitions, which form nonequilibrium electrons near the bottom of the conduction band ($E_g$ = 2.7 eV), but also Wannier–Mott excitons. The nonequilibrium electrons and excitons relax mainly due to the electron–phonon interaction. Electron– electron collisions dominate in the case $\hbar\omega_{p1}$ = 5.5 eV. It can be seen that the photoinduced changes in the ZnSe film permittivity are significantly different at different values. At $\hbar\omega_{p2}$ = 2.75 eV the photoinduced red shift of cavity modes is much larger than at $\hbar\omega_{p1}$ = 5.5 eV, which can be seen well when comparing Figs 2b and 2a. This is most likely related to the exciton contribution to the change in $\varepsilon(\omega)$.

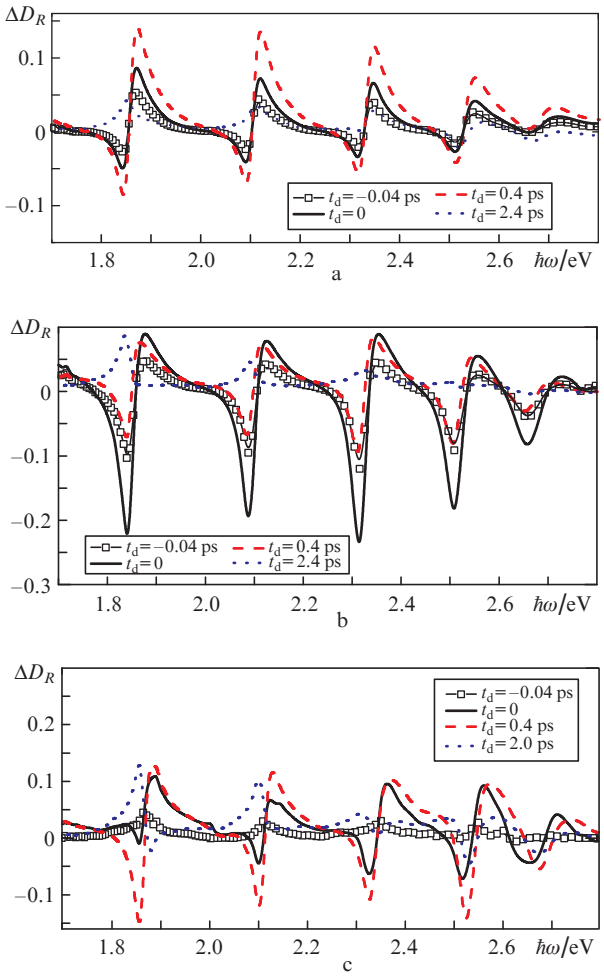


**Figure 2.** Spectra $\Delta D_R(\hbar\omega)$ of a 820-nm-thick ZnSe film on chromium at different delay times $t_d$ and pump photon energies of (a) 5.5, (b) 2.75, and (c) 2.34 eV for $E_g$ = 2.7 eV.

Note that the difference photoinduced response manifests itself even at a negative delay time ($t_d$ = –40 fs), when the supercontinuum probe pulse advances the pump pulse and its trailing edge is overlapped in time with the pump pulse leading edge. Note also that the initial stage of photoinduced response occurrence was observed in difference reflection spectra for a time shorter than the microcavity mode settling time (time of multiple light transmission through the film). The photoinduced response of cavity modes increases up to a delay time of 400 fs, and the cavity modes return to the initial position approximately 2 ps after; hence, the thermalisation time of photoexcited carriers in the samples under study does not exceed 2 ps.

## 3. Subband excitation ($\hbar\omega_p < E_g$)

In contrast to supraband excitation, under subband excitation ($\hbar\omega_p < E_g$) a light pulse passes through a ZnSe film with-

out being absorbed in single-photon processes and excites electrons in a thin surface metal layer at the interface with the semiconductor. The excitation of metal electrons manifests itself primarily in a rise in the damping coefficient $\gamma_{pm}$ of metal plasmons, i.e., in the change in the boundary conditions for the cavity modes and, first of all, in the increase in the imaginary part of permittivity $\varepsilon_m(\omega)$ of metal and, therefore, increase in the intensity of absorption bands of interference modes of the semiconductor film on metal [4, 5]. The behaviour of cavity modes under subband excitation was investigated in ZnS and ZnSe films of different thicknesses, located on different metal substrates: Cu, Ni, and Cr [7–15]. The most interesting turned out to be the results of studying the femtosecond dynamics of cavity modes under subband excitation in only ZnSe films on chromium. For the ZnS and ZnSe films on copper and nickel substrates, the difference spectra $\Delta D_R(\hbar\omega)$ were unipolar at all delay times $t_d$, a fact indicating that the cavity modes do not shift under excitation, and it is only the cavity-mode absorption intensity that changes. As was shown in [4], the light absorption coefficient of a film on metal at the frequencies of interference modes is determined by the imaginary part of metal permittivity. The cavity-mode absorption intensity also increases with an increase in $\mathrm{Im}[\varepsilon_m(\omega)]$.

The spectra $\Delta D_R(\hbar\omega)$ of a ZnSe film on chromium in different instants are shown in Figs 2b and 3 (in more detail). The pump photon energy was $\hbar\omega_{p3} = 2.34$ eV, and the pulse energy was 1.5 μJ. The width of the pump pulse and supercontinuum (1.6–3.2 eV) probe pulse was 50 fs. The spectral range under consideration contains four cavity modes. The linear RO spectra of a 820-nm-thick ZnSe film on chromium for $\omega < \omega_{ex} \leqslant E_g$ 2.7 eV are also presented in Fig. 3 (top). At negative $t_d$ values the probe pulse arrives at the film before the pump pulse. The repetition frequency of pump and probe pulses was 2 Hz, and the $t_d$ value was varied with a step of 7 fs in the range from –200 fs to ~2.5 ps. The probe pulse is not overlapped with the pump pulse at $t_d = -200$ fs, and the RA spectrum of the probe pulse is that of unexcited sample.

The pattern for ZnSe films on chromium is more interesting than for ZnSe films on nickel and copper. At delay times ranging from –70 to –42 fs, as can be seen in Fig. 3, the spectrum $\Delta D_R(\hbar\omega)$ has a practically constant sign, as well as for the films on nickel and copper [7–14]. The main physical processes characteristic of subband excitation and the characteristic hierarchy of times were considered in [9]. A series of fast processes induced by the pump pulse occur in a thin metal layer (at the extinction depth) near the interface with the semiconductor; the characteristic times of these processes range from several femtoseconds to several tens of picoseconds.

The main ones are as follows: excitation of electrons in the metal, which leads to a change in the boundary conditions for the microcavity eigenmodes; tunneling of nonequilibrium carriers from the metal into the semiconductor; two-photon absorption in the semiconductor layer; and heating of the structure. All these processes can be detected from photoinduced responses of cavity modes. The fastest process, which occurs even in the femtosecond range at the pulse leading edge, is the photoexcitation of nonequilibrium carriers in the metal. Then a partial thermal equilibrium is established in the electron subsystem for times longer than the electron–electron interaction times: several tens of periods of plasma oscillations of metal conduction electrons, i.e., for times on the order of several tens or several hundreds of femtoseconds. Furthermore, due to the electron–phonon interactions, excited electrons emit phonons, and equilibrium is established in the electrons–lattice system for times on the order of several picoseconds.

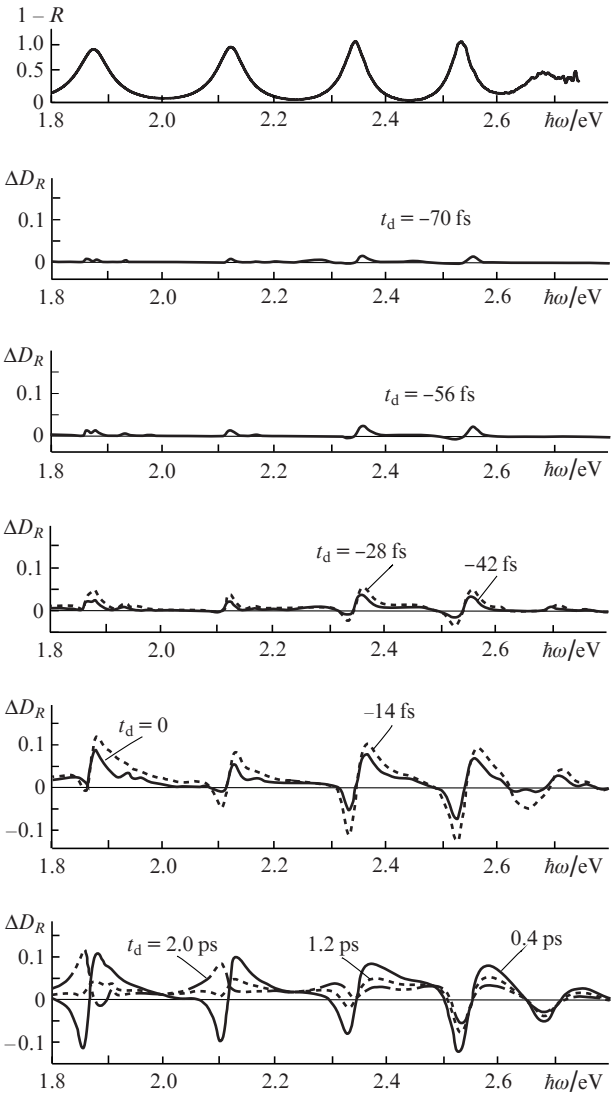


**Figure 3.** RA spectrum (top) of a 820-nm-thick ZnSe film on chromium and the spectra $\Delta D_R(\hbar\omega)$ of this film at different delay times $t_d$ [13, 14]. The pump photon energy $\hbar\omega_{p3} = 2.34$ eV.

For times on the order of electron–electron collision time, the most pronounced changes in the electron distribution function are observed near the Fermi level; as a result, the changes in the metal permittivity are most pronounced at the frequencies corresponding to the transitions to the Fermi level vicinity [4, 7–14]. The main contributions to the difference optical density $\Delta D_R(\hbar\omega)$ are from the changes both in the imaginary part of metal permittivity $\varepsilon_m$ and the semiconductor permittivity $\varepsilon_2(\omega)$. Some of the nonequilibrium carriers in the metal, excited by an ultrashort pulse (or its leading edge), may penetrate the semiconductor (either passing above the Schottky barrier or tunnelling through it [4, 8–14]) and thus increase $\varepsilon_2(\omega)$. If the electron velocity on the metal Fermi surface is $V_F \approx 10^8$ cm s$^{-1}$ and the thickness of the metal layer excited by the pump pulse is $l_{ex} \approx 2/\alpha_m(\omega) = 20–30$ nm ($\alpha_m$ is the absorption coefficient of metal), the electron time of flight

through the barrier can be estimated as ~10 fs. This estimate is in good agreement with the observed difference response (Fig. 3) both for negative delays ($t_d < -40$ fs), when the response is determined by the change in the chromium permittivity, and for $t_d \approx 0$, when the response is determined by the change in the semiconductor permittivity.

After establishing quasi-equilibrium in the electron subsystems of both the metal and semiconductor, the Schottky barrier becomes impermeable for most of quasi-equilibrium electrons [9–14]. The concentration of injected electrons will be proportional to the density of states in the metal at the Schottky barrier height. The density of allowed electronic states above the Fermi surface (at the Schottky barrier height) is close to zero for nickel and copper but fairly high for chromium [16], which guarantees possibility of electron injection from the chromic substrate into the semiconductor. The Schottky barrier height at the interface between an n-type semiconductor and a metal is ~1 eV, and the pump photon energy is sufficient to overcome the Schottky barrier for ZnSe on chromium but insufficient for ZnSe on copper and nickel. The nonequilibrium carriers injected into the semiconductor change its permittivity. During the excitation pulse electrons from the metal penetrate the semiconductor at a depth of several tens of nanometres and become distributed over the entire film volume for ~1 ps. The injection time is limited by the electron–electron relaxation time [9–11].

For delays $0 < t_d < 2$ ps (Fig. 3), the spectra $\Delta D_R(\hbar\omega)$ exhibit an alternating signal, which reaches a maximum in amplitude at $t_d \approx 0.1$ ps and then relaxes with a characteristic time of ~1 ps to a constant-sign signal. The two-polar signal of the photoinduced difference response is very similar to the first derivative of the linear absorption spectrum of structures at interference mode frequencies (see Fig. 1). This fact is indicative of a spectral shift of cavity mode bands under excitation by femtosecond laser pulses. The frequency shift for the interference mode of plane-parallel insulator layer on a metal is primarily possible because of the ultrafast change in the electron distribution function, which leads (for times exceeding the electron–electron collision times) to a change in the semiconductor film permittivity, and (at a smaller extent) to a change in the metal plasmon frequency [4, 9].

Thus, in the initial stage of subband excitation, the pump-pulse leading edge excites electrons at the extinction depth of the metal, changing its permittivity and the boundary conditions for cavity modes. This leads to an increase in absorption at the cavity mode frequencies and broadening of the absorption lines. Then electrons from the metal penetrate the semiconductor and change its permittivity, and therefore, the microcavity optical thickness, which gives rise to a frequency shift for cavity modes. Note that the recorded signal contains not only a contribution of the induced reflection from the surface and interface but also a contribution of photoinduced absorption in the semiconductor, because the excitation and probe pulses pass twice through the film. There may be an additional contribution (for a time on the order of pulse duration) to the change in the difference optical density at zero delay times, which is related to the two-photon absorption in the semiconductor.

Note that second-harmonic generation may also occur at the metal–semiconductor interface; the single-photon absorption of the second harmonic in the semiconductor should lead to the same effects as the two-photon absorption. The spectral dependence of two-photon absorption is directly related to the microcavity eigenmodes and repeats the shape of the linear absorption spectrum of the sample. The two-photon absorption changes the semiconductor permittivity. This contribution competes with the aforementioned contributions under subband excitation, which is in qualitative agreement with the experimentally obtained difference optical density at delay times close to zero.

## 4. Conclusions

Femtosecond laser pulses can be used to manipulate selectively the boundary conditions for microcavities; control interference modes; and modify the temporal, spectral, and spatial characteristics of nanostructures of the semiconductor-on-metal type. The measurement of the frequency shift of interference (cavity) modes is a very sensitive method for studying the ultrafast photoinduced processes at the semiconductor film–metal interface, which makes it possible to establish in some cases the time hierarchy of different processes occurring at the interface and in the semiconductor film on metal. An excitation of such a structure by a femtosecond laser pulse leads to a series of ultrafast processes, which cause photoinduced changes in the permittivity of both the semiconductor film and metal substrate. This circumstance opens up certain prospects of application of these structures not only as an element base for optoelectronics but also in fundamental investigations of ultrafast electrodynamic and photodynamic processes [1, 17, 18].

***Acknowledgements.*** I must recall that the above-described study, performed at the Laboratory of Femtosecond Spectroscopy of the Institute for Spectroscopy of the Russian Academy of Sciences, was actively supported by V.S. Letokhov. I am also grateful to the researchers from this laboratory: Yu.A. Matveets, S.V. Chekalin, A.L. Dobryakov, V.M. Faztdinov, and V.O. Kompanets for carrying out experiments and to Yu. E. Lozovik for the theoretical contribution to understanding of the physical processes occurring in our experiments.

## References

1. Berman P.R. (Ed.) *Cavity Quantum Electrodynamics* (Boston: Academic, 1994).
2. Dobryakov A.L., Golubev V.V., Letokhov V.S., Lozovik Yu.E., Matveets Yu.A., Stepanov A.G., Farztdinov V.M., Chekalin S.V. *Opt. Spektrosk.*, **76** (6), 975 (1994).
3. Kovalenko S.A., Ernsting N.P., Ruthmann J. *Chem. Phys. Lett.*, **258**, 445 (1996).
4. Vinogradov E.A. *Phys. Usp.*, **45** (12), 1213 (2002) [*Usp. Fiz. Nauk*, **172** (12), 1371 (2002)].
5. Vinogradov E.A. *Phys. Rep.*, **217** (4), 159 (1992).
6. Troitskii Yu.V. *Mnogoluchevye interferometry otrazhennogo sveta* (Multibeam Reflected-Light Interferometers) (Novosibirsk: Nauka, 1985).
7. Vinogradov E.A., Farztdinov V.M., Dobryakov A.L., Kovalenko S.A., Lozovik Yu.E., Matveets Yu.A. *Laser Phys.*, **8** (1), 316 (1998).
8. Vinogradov E.A., Farztdinov V.M., Kovalenko S.A., Dobryakov A.L., Lozovik Yu.E., Matveets Yu.A. *Laser Phys.*, **9** (1), 215 (1999).
9. Vinogradov E.A., Dobryakov A.L., Kovalenko S.A., Lozovik Yu.E., Matveets Yu.A., Farztdinov V.M. *Izv. Ross. Akad. Nauk, Ser. Fiz.*, **63** (6), 1056 (1999).
10. Vinogradov E.A., Davis C.C., Dobryakov A.L., Lozovik Yu.E., Smolyaninov I.I. *Laser Phys.*, **10** (1), 76 (2000).

11. Vinogradov E.A., Dobryakov A.L., Lozovik Yu.E., Matveets Yu.A. *Laser Phys.*, **11** (11), 1147 (2001).
12. Vinogradov E.A., Lozovik Yu.E. *Izv. Ross. Akad. Nauk, Ser. Fiz.*, **68** (1), 25 (2004).
13. Vinogradov E.A., Lozovik Yu.E. *Phys. Status Solidi C*, **2** (2), 791 (2005).
14. Vinogradov E.A. *Laser Phys*., **15** (7), 954 (2005).
15. Vinogradov E.A., Kompanets V.O., Lozovik Yu.E., Matveets Yu.A., Chekalin S.V. *Izv. Ross. Akad. Nauk, Ser. Fiz*., **72** (5), 715 (2008).
16. Kulikov N.I., Alouani M., Khan M.A., Magnitskaya M.V. *Phys. Rev. B*, **36** (2), 929 (1987).
17. Lozovik Yu.E., Tsvetus V.G., Vinogradov E.A. *Phys. Scr*., **52**, 184 (1995).
18. Dodonov V.V., Dodonov A.V. *J. Russ. Laser Res.*, **26** (6), 445 (2005).